Global and Planetary Change 157 (2017) 244–258

Contents lists available at ScienceDirect

Global and Planetary Change

journal homepage: www.elsevier.com/locate/gloplacha

A comparison of simultaneous temperature and humidity observations from the SW and NE slopes of Kilimanjaro: The role of slope aspect and differential land-cover in controlling mountain climate

Nicholas C. Pepin*, Gary Pike, Martin Schaefer, Clare M. Boston, Harold Lovell

Department of Geography, Buckingham Building, Lion Terrace, University of Portsmouth, PO1 3HE, UK

ARTICLE INFO

Keywords:
Mountain climate
Air temperature
Relative humidity
Upslope moisture transport
Land cover change
Ice fields

ABSTRACT

The recession of the current ice fields near the summit of Kilimanjaro has been shown to be controlled largely by climate. Despite detailed research into summit climate, including mass and energy balance modelling, understanding Kilimanjaro as a whole has been limited by lack of observations on the mountain slopes. Analysis of hourly air temperatures, relative humidities and vapour pressures from 22 weather stations installed between September 2012 and 2015 across the mountain from south-west to north-east are presented for the first time. Moisture is shown to move upslope on both sides of the mountain during the afternoon. The north-east slope is less humid and warmer on average than the south-west slope. Temperature differences between slopes reach 4–5 °C during the morning in the rainforest zone (2000–2500 m) and on the crater wall (5000–5550 m). Slope differences are broadly similar in size to local contrasts within the south-west slope caused by the rainforest (at 1890 m) and ice fields (at 5800 m). Although both slopes show similar moisture regimes, there are contrasts in moisture content particularly in the zone just above the current rainforest limit (3000–3200 m). This decoupling extends up to 5000 m in the afternoon because the upslope transport of moisture is both weaker and delayed on the NE slope. At night the upper slopes are highly correlated implying that free-air moisture is the dominant source. Very moist events at crater level tend to be associated with widespread moistening across the whole mountain. These results can be used both to argue for and against the role of deforestation being an important influence on summit climate and therefore ice field recession.

1. Introduction

Kilimanjaro is the largest free standing mountain in Africa, reaching a peak of 5895 m (above sea level) and emerging from a surrounding plain at ~1000 m. The summit region is high enough to be one of the few locations near the equator covered with snow and ice. Recent research has largely been concerned with the decline in the summit ice fields over the last century or more (Hastenrath and Greischar, 1997, Mölg et al., 2003, 2008, 2009b, Mölg and Kaser, 2011). The most recent estimate for the date of disappearance of current summit ice is 2040 (Cullen et al., 2013). The reasons for the current decline are a consequence of changes in the mountain climate, particularly a drying of the upper atmosphere (Mölg et al., 2008, 2010; Kaser et al., 2010), which has resulted in a negative mass balance due to increased sublimation and reduced accumulation.

Although there are good records of weather observations on the summit ice field itself (Mölg and Hardy, 2004), there has been less analysis of conditions on the mountain slopes. In the tropics especially, mountains act as an integrated system. The slopes act as a heat source in the daytime, becoming warmer than the free atmosphere (Richner and Phillips, 1984; Pepin and Seidel, 2005), which allows air to flow upslope through the formation of a thermal circulation. The reverse occurs at night when the slopes cool in comparison with the free atmosphere and air sinks downslope. The summit region therefore is subject to import of moisture from the lower slopes during the day. Despite past work demonstrating daytime upslope vapour transport based on a transect of 10 stations on the south-west (SW) slope (Pepin et al., 2010), there has been no detailed comparison with processes on other slopes of the mountain due to a lack of data.

This paper examines climate data from the north-east (NE) side of the mountain for three years (2012–2015) and for the first time compares this with simultaneous observations from the SW slope (Fig. 1). The coherence in temperature patterns and moisture transport on the two sides of the mountain is examined. In particular, we examine contrasts between the slopes that result from the differential timing of and amount of direct solar radiation, and from land-cover differences.

* Corresponding author.
E-mail address: nicholas.pepin@port.ac.uk (N.C. Pepin).

http://dx.doi.org/10.1016/j.gloplacha.2017.08.006
Received 1 February 2017; Received in revised form 1 August 2017; Accepted 8 August 2017
Available online 09 August 2017

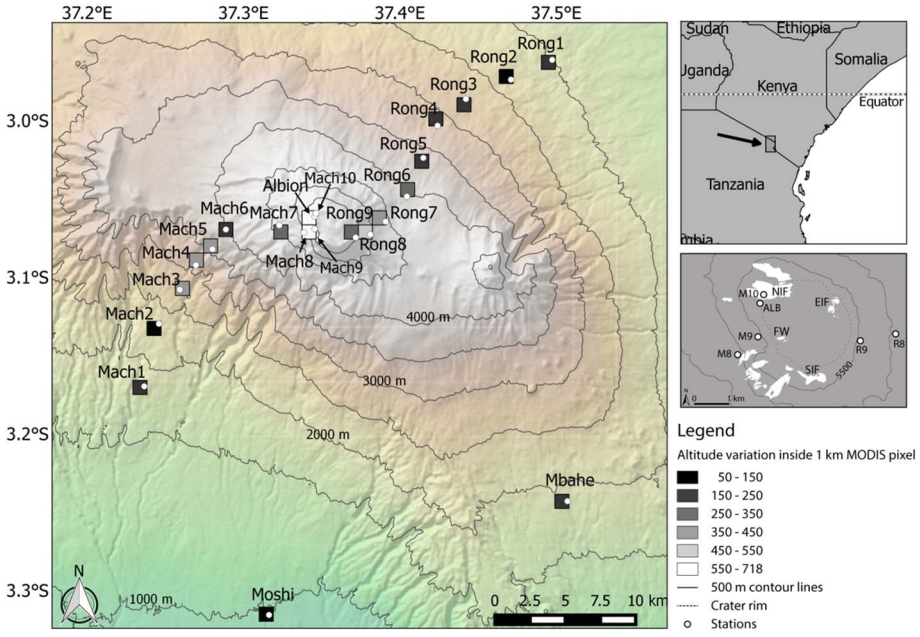

Fig. 1. Map showing the location of 22 temperature stations across Kilimanjaro. The SW slope stations are named Mach1–Mach10 (ice field) and the NE stations Rong1–Rong9 (crater wall). Additional stations are situated at Moshi (991 m), Mbahe Farm (1839 m) and Albion (5794 m). The squares represent 1 km × 1 km MODIS pixels used for the cloud mask (see text). Stations are located on the Rongai (Rong) and Machame (Mach) trekking routes. Inset shows the summit stations and location and size of the ice fields in 2015 (NIF = Northern Ice Field, SIF = Southern Ice Field, FW = Furtwangler Glacier, EIF = Eastern Ice Field).

The NE slope receives direct sunlight much earlier in the day and heats up more quickly than the SW slope. By the time the sun has moved round to the western slope during the afternoon, cloud build-up is usually substantial (Meyer, 1890, 1891), and this leads to an asymmetry in the current climate, causing glaciers to extend to lower elevations (~5000 m) on the western slopes compared to being constrained to the crater rim (> 5500 m) in the east (Gillman, 1923; Cullen et al., 2013). The rainforest zone is well-developed on the SW slope, with extensive rainforest extending from 1800 to 3000 m. By contrast, the NE slope is much drier and has a relatively small forest zone (~2200–2500 m). In addition, deforestation for crop cultivation is taking place on the NE slope immediately outside the national park (~2000 m) near the Rongai Gate and coniferous plantations have replaced the natural rainforest in many areas on this side of the mountain (Altmann et al., 2002).

This paper first examines the mean diurnal signals of air temperature, vapour pressure and relative humidity at all stations (comparing each slope) before examining elevational, diurnal and seasonal patterns of slope differences. Local scale differences created by vegetation at the rainforest edge (at 1890 m) and the Northern Ice Field (NIF) (at 5800 m) provide context to understanding the importance of these slope differences. The NE slope is shown to be warmer and drier (less humid) in general. We also use satellite data to examine cloud differences between the two slopes, and compare these with observed differences in relative humidity. Most of the heavy snowfall at crater level that contributes to ice accumulation falls in a few events. Therefore the next section examines conditions on the mountain slopes for days on which frequent cloud and/or snowfall was observed at crater level (n = 40). This shows how conditions on the rest of the mountain correlate with these high intensity precipitation events at summit level. This analysis allows us to discuss the relevance of the observed slope moisture patterns for the current summit ice-field mass balance and, through comparison with modelling studies, to draw conclusions about the effects of slope aspect and land-cover contrasts on summit climate.

1.1. The climate and ice fields of Kilimanjaro

The climate of Kilimanjaro was of interest in the 19th century when explorers first climbed the mountain (Meyer, 1890, 1891), with the reported presence of snow on a mountain in the tropics/at the equator leading to intense debate (Cooley, 1852; Bridges, 1976). Following this, the first model of the thermal circulation on a tropical mountain was put forward by Troll and Wien (1949) based on Mount Kenya and has since been adapted for Kilimanjaro (Duane et al., 2008; Mölg et al., 2009a). This showed that most of the moisture is on the lower slopes of the mountain, trapped below a semi-permanent temperature inversion around 3000 m (Findlater, 1977). Thus, rainfall peaks around 2200 m at 2000–3000 mm per year dependent on location (Røhr and Killingtveit, 2003; Schuler et al., 2014). The wettest slopes face south and south-west (Hemp, 2006) which is strange given that the prevailing winds in the upper atmosphere are from the east. However, the southern and western flanks of the mountain are thought to be prone to moisture convergence which is dynamically forced (Mölg et al., 2009a). During the day, solar heating causes upslope air movement on all slopes which transfers moisture upwards towards the summit crater. However, at higher altitudes frequent strong northerly or easterly winds often prevent the moisture on the SW slope from reaching crater level, the mechanical free-air strength suppressing the upslope flow (Whiteman, 1990), and elevations above 4500 m are therefore arid. The free air itself is extremely dry, and it is surprising that under such present conditions any ice fields exist on the crater at all. They would certainly not form in today's climate (Kaser et al., 2004) and are therefore thought to be a remnant of a much moister regime in the near past (Kaser et al., 2010).

There has been extensive effort to assess both the current rate of recession of the summit ice fields (Cullen et al., 2006; Winkler et al., 2010; Cullen et al., 2013; Pepin et al., 2014; Bohleber et al., 2016) and the causes of this, in particular the relative importance of the various climate influences (air temperature, precipitation, cloud patterns, solar radiation) (Mölg and Hardy, 2004; Mölg et al., 2008, 2009b). Most of the work has been concerned with the Northern and Southern ice fields (NIF and SIF) (Fig. 1 inset) which are the largest ice masses remaining (as at 2015). Although temperatures have increased over the last century (Stocker et al., 2013), not least due to anthropogenic enhancement of the greenhouse effect, the mean air temperatures at crater level remain well below freezing (Duane et al., 2008; Mölg and Hardy, 2004; Mölg et al., 2009b), with sublimation dominating over melting in the mass balance equation (Mölg et al., 2008). Therefore the main cause of current decline is largely agreed to be a drier climate, with direct solar radiation playing a pivotal role in controlling ice-field morphology of the NIF for example (Winkler et al., 2010; Pepin et al., 2014). The importance of moisture in dominating mass balance is broadly similar

to Mount Kenya, even though temperatures there at glacier elevations are slightly warmer (Prinz et al., 2016). The causes of drying in East Africa are thought to be related to changes in Indian Ocean sea-surface temperatures (SSTs) (Chan et al., 2008; Mölg et al., 2009b), even though many future climate models predict wetter conditions in general (see Shongwe et al., 2011, Cook and Vizy, 2013). There has also been research into the influence of deforestation on the mountain slopes (Fairman et al., 2011; Mölg et al., 2012), but despite modelling efforts, the extent to which local scale (e.g. deforestation) and/or regional scale factors (e.g. changing SSTs) are contributing to the drying climate is still unclear. The prevailing wind is from the east so the free air is indeed influenced by the Indian Ocean, especially during the wet seasons, but how this free air interacts with the mountain is still not fully understood (Mölg et al., 2009a; Pepin et al., 2010).

The main peak of Kilimanjaro (Kibo) (Fig. 1) is an isolated cone and as such the air does not tend to flow over the summit crater but around it, with the windiest locations being on the NW and SE sides where the air is funnelled as part of a split flow pattern (Schär, 2002; Mölg et al., 2009a). The saddle between Kibo and Mawenzi on the east side of the summit crater is particularly prone to strong northerly winds as a consequence. Since the southern (and SW) slopes of the mountain are much moister than the northern (and NE) side (Coutts, 1969), the traditional orographic model with opposing windward and leeward effects (Daly et al., 1994; Roe, 2005) is not appropriate. Added to the isolated cone-like topography is the fact that the air is typically stable above the trade wind inversion (Hastenrath, 1991) and this, along with relatively weak upper level flow (in comparison with mid-latitudes), prevents substantial orographic rainfall from developing, at least in the traditional sense. Conversely, the heaviest precipitation at crater level appears to form when upper level winds are weak, which allows the thermal heating of the mountain slopes to draw up moisture from the lower slopes. However, whether this is a symmetrical process on all slopes is not known. Particularly intense rainfall is sometimes recorded on the upper parts of the SW slope where convergence between the upper level split flow and a thermal upslope flow can develop (Mölg et al., 2009a).

The mountain lies almost on the equator and thus sunrise is at approximately 0630 and sunset at 1830 EAST (East African Standard Time) throughout the year. The daily cycle in both temperature and humidity is more influential than the annual one, although there are two distinct wet seasons. The long rains fall between March and May and bring heavy rainfall to all elevations (Camberlin and Phillipon, 2002), and the short rains occur in November and December but are more showery (convective) in nature. The atmosphere remains unstable into the January/February dry season, and lapse rates on the mountain are much steeper at this time (Duane et al., 2008). The most stable period is the long dry period from July to September/October when cloud-free conditions are common above a mid-level temperature inversion around the treeline (3000 m).

A fundamental limitation to a more detailed understanding of mountain climate on Kilimanjaro has been the lack of climate observations from across the whole mountain. There are high quality weather stations on the NIF (Mölg and Hardy, 2004), and also next to its vertical walls (Winkler et al., 2010). Thus, the local energy balance on the ice field and some adjacent slope glaciers is fairly well understood (Mölg et al., 2003; Cullen et al., 2007; Mölg et al., 2008, 2009b, 2009c). In addition to summit observations, one transect of weather stations was installed on the SW slope in 2004 (Machame route), which enabled the tracking of moisture up that slope (Duane et al., 2008), and there are also some temperature and precipitation observations between 1900 m and 3200 m nearby on the southern slopes (Schuler et al., 2014). A large number of stations have been installed recently as part of ecological monitoring on the southern slopes up to around 4000 m (Appelhans et al., 2016). Their comparison with our original SW transect (Duane et al., 2008) shows broadly similar seasonal and elevational patterns in temperature (e.g. lapse rates) and similar moisture decline and increase in moisture variability towards higher elevations. Until recently, as far as we know there have been no systematic observations on the NE side of the mountain and there is no study covering the whole elevational range from plains (~1000 m) to summit crater (5800 m). The NE slope (Rongai route) (Fig. 1) can be viewed as the windward slope, and the SW slope (Machame route) as the leeward. There are only slight variations between the seasons. During the austral summer/winter the upper flow has more of a northerly/southerly component, but during both wet seasons (MAM and OND) upper level flow comes most frequently from the sector 45–90° (Fairman et al., 2011; Mölg et al., 2009a).

2. Methods

22 stations (9 on each slope, 2 in the crater and 2 on the surrounding plains) were instrumented using Hobo Pro v2 U23-001 data loggers measuring air temperature and relative humidity every hour. Data runs from September 2012 to September 2015. All times are East African Standard Time (EAST or UTC + 3 h). Each transect runs from the plains (~1000 m) through the six ecological zones characteristic of Kilimanjaro (Fig. 2) up to and including the summit crater (5800 m). These zones include a) cultivated belt, b) montane cloud forest (rainforest), c) giant heather, d) alpine moorland, e) alpine desert and f) ice field. Sensors were placed at approximately 400 m elevational intervals on each slope, and at equivalent elevations on each side of the mountain (Table 1 and Fig. 1) to enable easy comparison. However, this means that sensors at equivalent elevations may not always be in the same ecological zone because zones are somewhat compressed on the NE slope.

Data loggers were screened using white PVc tubing open at both ends, with the open ends facing north and south to prevent direct solar radiation from entering the tube. All measurements were taken at 2 m above ground level. The (almost) horizontal angle of the tube prevents reflected radiation (from snow or the ground) reaching the sensor, but prevents air from stagnating in the tube. This method of screening has been tested through calibration against an aspirated shield at the summit station on the NIF (see Fig. 2f for equipment set-up) and differences in observations were minimal (Duane et al., 2008). The data logger specification has been assessed by Whiteman et al. (2000) as suitable for local scale climate monitoring. Typical sensor accuracy is quoted as ± 0.21 °C from 0 to 50 °C.

After basic diurnal patterns on each slope are examined, the difference between the two slopes is calculated by subtracting the NE station value from the SW station (at the equivalent elevation). With the exception of the first station on each transect, elevation differences are very small (Table 1) and thus have not been compensated for. Positive/negative temperature differences mean that the SW slope is warmer/cooler, and positive/negative relative humidity or vapour pressure differences mean that the SW slope is moister/drier. Vapour pressures were calculated using the equations of Kuemmel (1997) above a water surface. Cloud frequencies were estimated using observed relative humidity data (RH > 95%) and also obtained from MODIS MYD11A2 LST cloud mask data (AQUA) for the 1 km pixels (Fig. 1) corresponding to the weather stations (for more details see Pepin et al., 2016).

At Albion station on the crater (5794 m), a downward facing Hobo Pendant light sensor measured reflected shortwave radiation. Values over 30,000 Lux (237 W/m^2) at 1100 EAST (when there is usually a lack of cloud) led to the day being classified as snow-covered (~43% of total days) (Pepin et al., 2016). A change from a non-snow covered day to a day with snow cover was identified as a day with significant snowfall at crater level (n = 40). Although there may be some uncertainty in this proxy measurement, rapid increases were usually extremely distinct, with reflected radiation dramatically increasing from one day to the next and then decreasing gradually over subsequent days. Significant snowfall days are thus easy to identify.

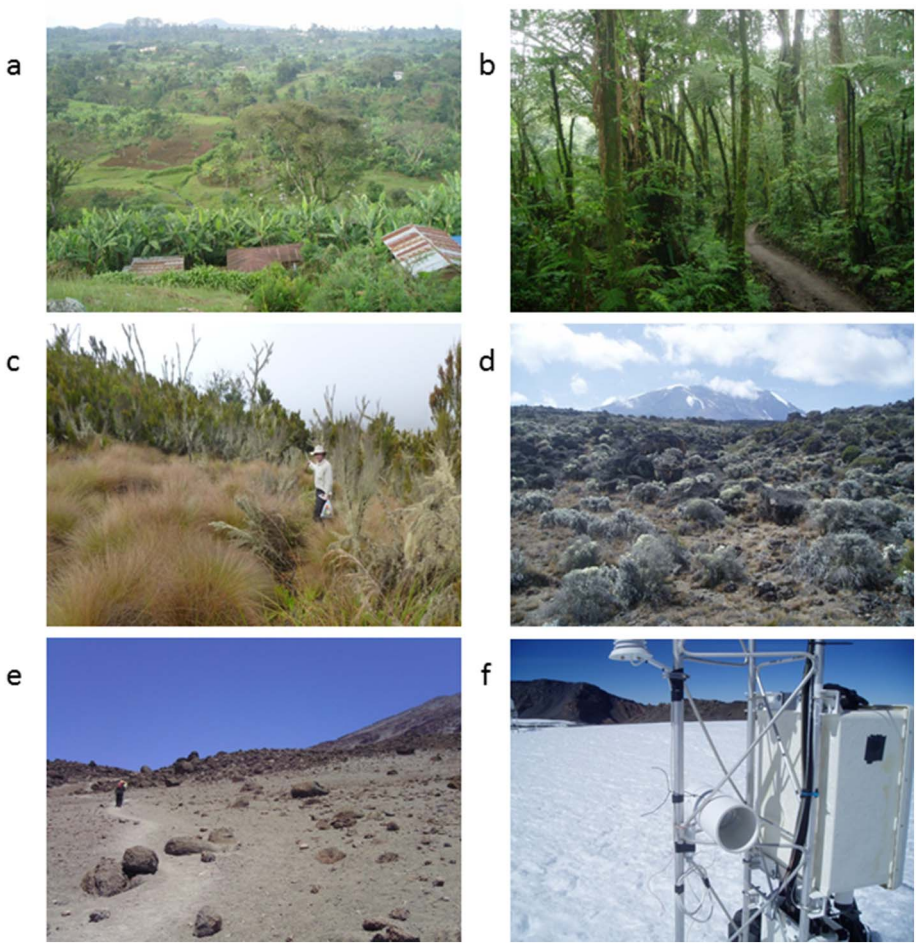

Fig. 2. Photographs of the vegetation zones of Kilimanjaro. a) cultivated belt (up to 1850 m), b) montane cloud forest (1850–3100 m), c) giant heather zone (3100–3900 m), d) alpine moorland (3900–4500 m), e) alpine desert (> 4500 m), f) ice field on summit crater (5800 m). Elevations of zones are given for the SW slope. Zones are slightly compressed on the NE slope. The data logger screening and set up is illustrated in Fig. 2f (horizontal PVc tube fixed to mast).

3. Results

3.1. Mean diurnal temperature/humidity patterns on each slope

A comparison of mean air temperatures for each slope based on the whole 3 year period shows that in general the NE slope is warmer, particularly by day, and that the freezing level reaches above Rong9 (5457 m) during the afternoon, in contrast to the SW slope where it remains at around 5500 m (Fig. 3). A similar slope comparison based on hourly mean vapour pressures (Fig. 4) shows that on both slopes there is a fairly regular

Table 1
Station details.

Station	Latitude °N	Longitude °E	Elevation metres	Missing data (%)	Pixel elevation metres	Elevation difference (SW-NE)	Vegetation zone
Moshi	− 3.316	37.316	991	0	989	n/a	Savannah
Mbahe	− 3.243	37.507	1839	0	1903	n/a	Cultivated
Mach1	− 3.170	37.237	1890	68	1871	− 120	Rainforest
Mach2	− 3.130	37.246	2340	11	2288	+ 2	Rainforest
Mach3	− 3.108	37.259	2745	47	2777	− 19	Rainforest
Mach4	− 3.092	37.270	3178	24	3137	+ 2	Heather
Mach5	− 3.082	37.280	3610	32	3527	− 36	Heather
Mach6	− 3.070	37.289	4039	17	3966	− 54	Moorland
Mach7	− 3.067	37.323	4555	17	4434	− 21	Moorland
Mach8	− 3.071	37.339	4973	26	5134	+ 7	Desert
Mach9	− 3.069	37.346	5469	7	5134	+ 12	Desert
Mach10	− 3.059	37.346	5803	0	5479	+ 9	Ice Field
Albion	− 3.061	37.346	5794	0	5479	+ 9	Desert
Rong9	− 3.075	37.372	5457	0	5636	+ 12	Desert
Rong8	− 3.073	37.381	4966	55	5188	+ 7	Desert
Rong7	− 3.065	37.391	4576	0	4688	− 21	Desert
Rong6	− 3.049	37.405	4093	0	3993	− 54	Moorland
Rong5	− 3.023	37.415	3646	33	3662	− 36	Moorland
Rong4	− 3.003	37.424	3176	22	3091	+ 2	Heather
Rong3	− 2.986	37.442	2764	0	2796	− 19	Heather
Rong2	− 2.974	37.471	2338	43	2372	+ 2	Rainforest
Rong1	− 2.961	37.498	2010	25	2032	− 120	Cultivated

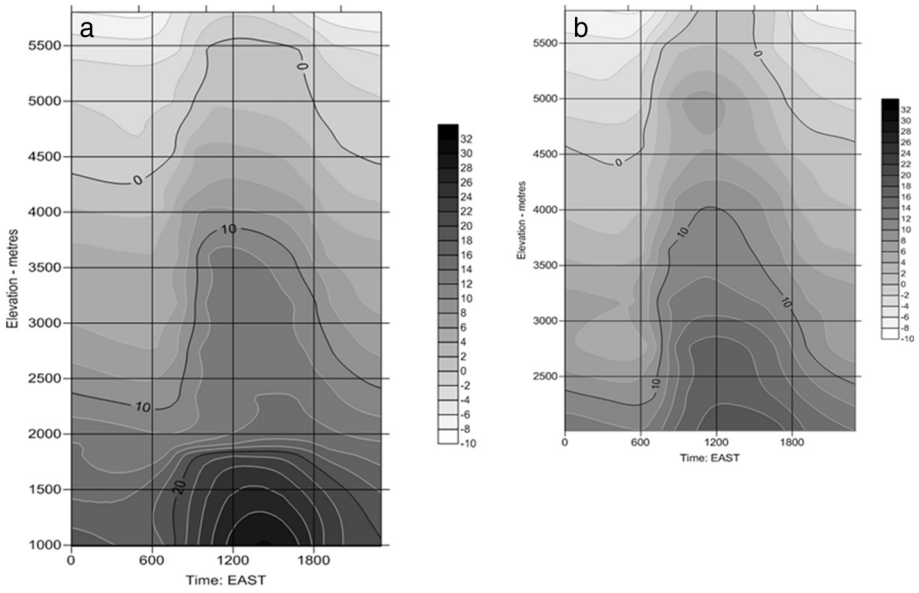

Fig. 3. Mean air temperature (°C) for each hour of the day for a) the SW slope and b) the NE slope, based on the stations on that slope only. Because the stations Moshi and Mbahe are to the SW of the mountain they are included in the SW panel which consequently extends to lower elevations. The same grey scale is used on both panels.

decrease in mean vapour pressure with elevation. However there is also an increase in vapour pressure during the day at all elevations, and vapour pressures are generally higher on the SW slope.

The difference between the two slopes of air temperature (panel a) and vapour pressure (panel b) over the mean diurnal cycle are shown in Fig. 5. The SW slope is generally cooler and moister than the NE. On average this would be expected because Kilimanjaro is in the southern hemisphere (thus slopes with a northerly component should be warmer), and also in a convective regime direct radiation will be suppressed on slopes facing the afternoon sun. The biggest cooling effect on the SW slope is seen around midday (1200 EAST) in the rainforest zone (2000–3000 m) but also there are large differences during the early morning at around 5000 m. At the higher elevation there is no vegetation, so aspect (including shading) effects on the crater wall must be responsible. Vapour pressure differences between the two slopes are mostly positive (i.e. moister on the SW slope) but there are some unexpected negative differences in the rainforest zone (2000–2500 m) during the morning and on the crater wall (~5000 m), mostly coinciding with areas which are also cooler on the SW slope.

Relative humidity provides a good representation of the likelihood of cloud cover since in theory cloud will form at station level when the relative humidity nears 100%. Our data (Fig. 6) demonstrates that mean relative humidities are particularly high on the SW slope, especially around 2000 m. The zone of almost perpetual cloud cover is displaced to slightly higher elevations (2500 m) on the NE slope and is much reduced in strength, especially in the afternoon. Both slopes also show a surge of moisture upslope in the afternoon, but relative humidities are much higher on the SW slope, the mean 80% isohume reaching over 5000 m from 1200 to 1800 EAST, as opposed to 4000 m on the NE slope. The moisture surge also appears somewhat later in the day on the NE slope, with humidities peaking as late as 1800 EAST around 3500–4000 m.

The mean diurnal cycle is represented for five elevation bands in Fig. 7 for air temperature (panel a), vapour pressure (panel b) and relative humidity (panel c). The ecological zonation is slightly different on the two slopes, the zones being compressed and at lower elevations on the NE side. Thus, as far as possible we have chosen elevation bands where the same zones overlap. Most locations are cooler and moister on the SW slope. This

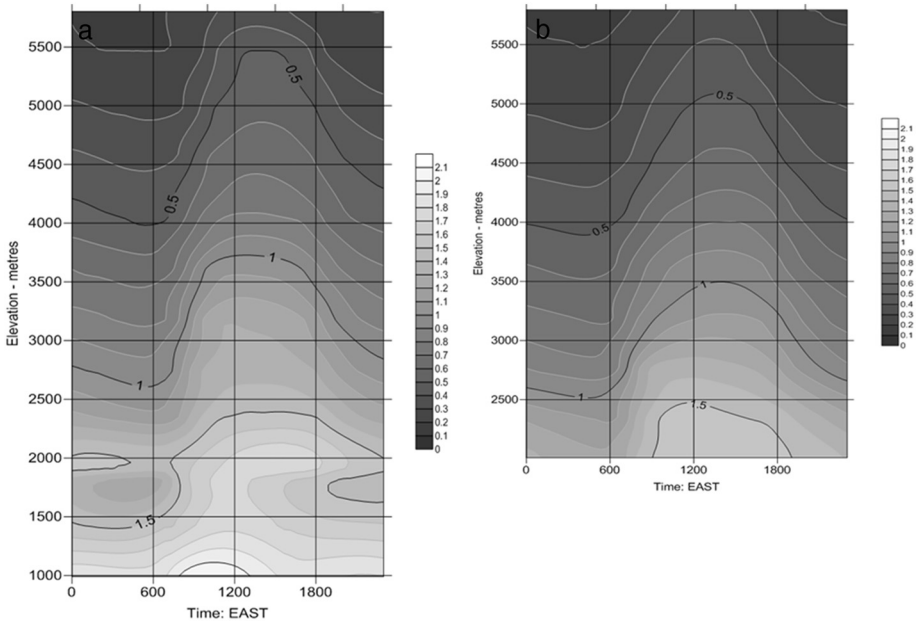

Fig. 4. Mean vapour pressure (kPa) for each hour of the day for a) the SW slope and b) the NE slope – similar format to Fig. 3.

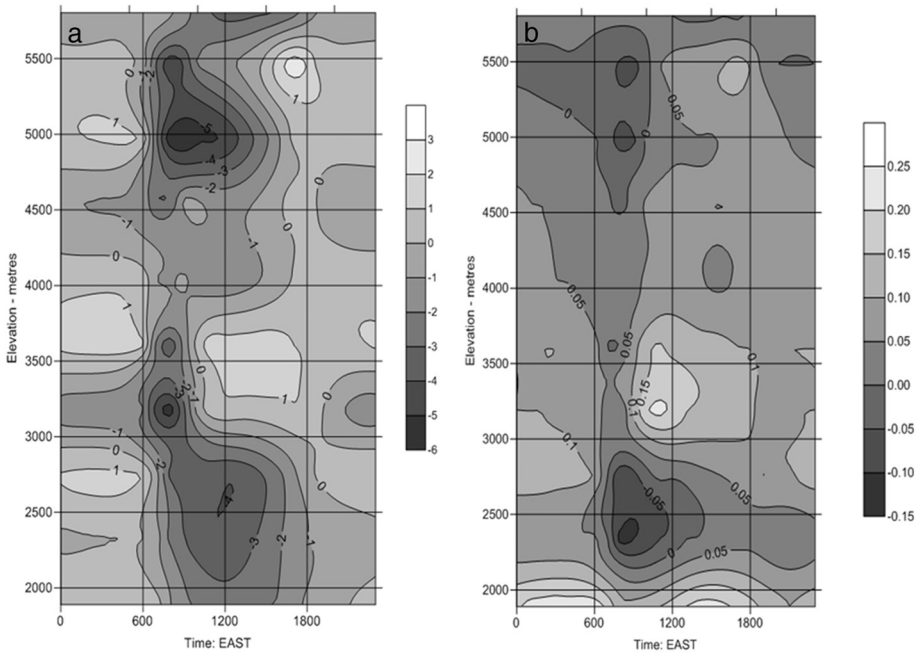

Fig. 5. Differences in a) air temperature (°C) and b) vapour pressure (kPa) between equivalent elevations on the SW and NE slope. Positive/negative values represent warmer/cooler and moister/drier conditions for the SW slope respectively.

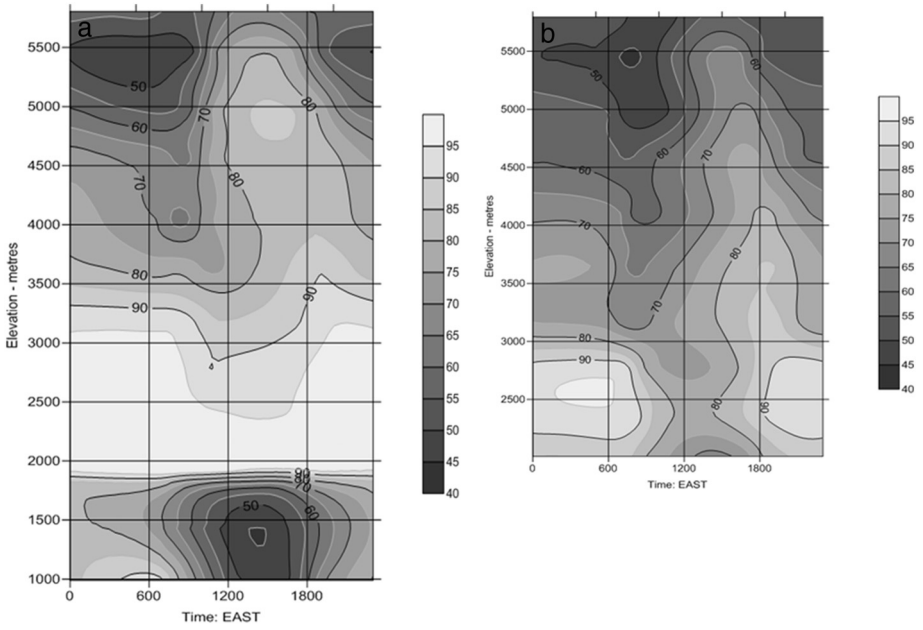

Fig. 6. Mean relative humidity (%) for each hour of the day for a) the SW slope and b) the NE slope – similar format to Fig. 3.

difference is not restricted to the rainforest zone (represented by 2339 m). Some of the largest differences in moisture are seen just above in the heather zone (3177 m), where the vapour pressure difference reaches a maximum of 0.2 kPa late morning, and relative humidity differences remain high all night. The strong positive difference in relative humidity at 3177 m implies a lower mean cloud base on the NE slope during the nocturnal hours. At a few elevations, namely the heather zone (3177 m), but also especially on the crater wall (5463 m), opposite contrasts in temperature can be seen early morning and late afternoon as the low angle sunlight will illuminate one slope but not the other. As expected, the NE slope is warmer in the early morning (0800 EAST) and SW slope in the late afternoon (1700 EAST).

Similar graphs were created for January (NE monsoon: austral summer), April (long rains), July (SE monsoon: austral winter) and October (Figs. 8–10). Temperature differences are broadly consistent throughout the year, although they are subdued during the long rains, and the high level aspect effects early and late in the day are strongest during July when there is a lack of cloud. The humidity differences are also broadly consistent between seasons, with the exception that the asymmetry in nocturnal cloud base (higher on the SW slope) tends to be enhanced in the July dry season. Daytime vapour pressure differences in the giant heather zone are largest during the NE monsoon (January) when the SW slope shows enhanced vapour pressure in comparison to the NE slope.

3.2. Local scale differences

To set some of the slope differences in context, we evaluate temperature and vapour pressure differences between

i) two stations at ~1890 m at the edge of the rainforest on the SW slope (Fig. 1): Mach1 (natural forest) and Mbahe (cultivated land) (Fig. 11a, b).

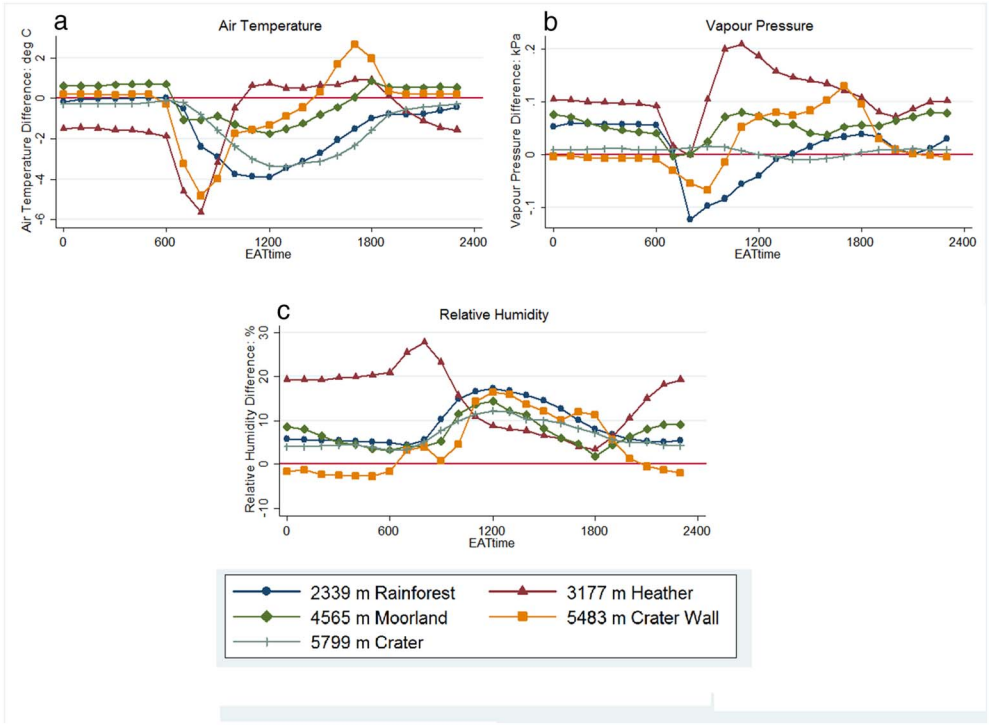

Fig. 7. Mean diurnal patterns in slope differences (SW minus NE slope) in a) air temperature (°C), b) vapour pressure (kPa), c) relative humidity (%). Five different elevation bands are shown. The summit difference represents the effect of ice versus no ice.

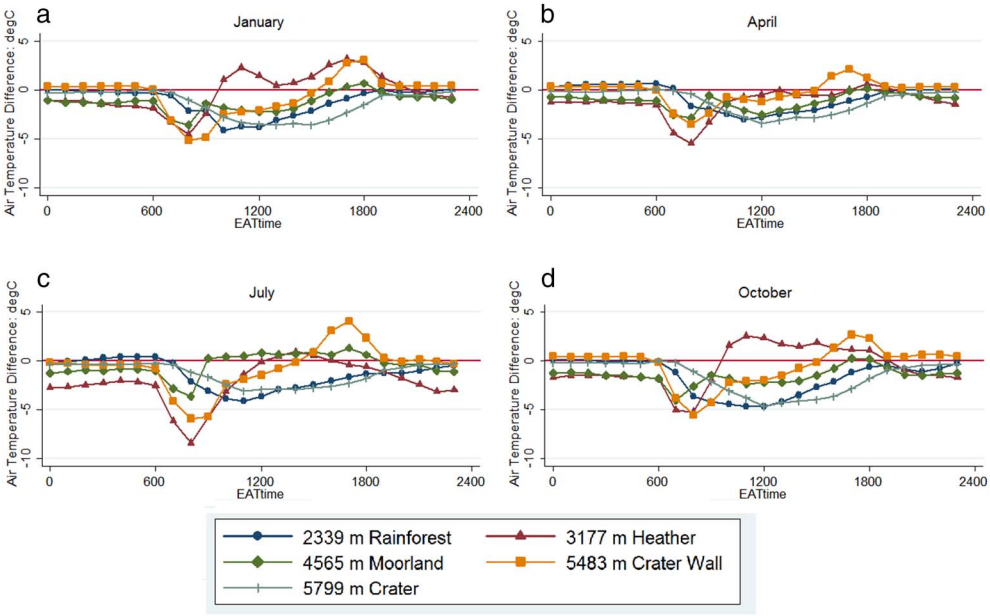

Fig. 8. Seasonal differences in diurnal patterns of slope differences (SW minus NE slope) in air temperature (°C) for a) January, b) April, c) July and d) October. Five different elevation bands are shown. The summit difference represents the effect of ice vs no ice.

ii) two stations on and off the ice field in the crater: Mach10 (on ice) and Albion (off ice) (Fig. 11c, d).

Elevation differences are small in both pairings. Both the rainforest and the ice field show strong diurnal signals in the size of the cooling effect with local cooling of 3–4 °C typical during the afternoon hours. At night, the rainforest is slightly warmer than the cultivated area, presumably due to reduction in longwave radiation loss due to canopy protection, but the ice field becomes approximately the same temperature as the non-ice area. When it comes to moisture differences however, the rainforest shows a daily signal (panel b), with a slight drying in the early morning changing to substantial moistening during the afternoon. The moister regime remains all night. During the wet season (April/May), the rainforest is moister all day, and night-time differences are sometimes up to 0.3 kPa. Moisture differences induced by the ice field (panel d) are much smaller (typically up to 0.03 kPa), and appear to be more strongly controlled by season rather than time of day. During the wet seasons (particularly March–May) the ice field is less moist than the comparable station off the ice, whereas during the long dry period of June–September the air above the ice field is moister than at the neighbouring station, suggesting that active sublimation is occurring. Interestingly this moisture excess above the ice field lasts all day and night, despite being of relatively small magnitude.

3.3. Relative humidity and cloud patterns

Cloud patterns are also obtainable through use of the MODIS cloud mask for the 8-day MYD11A2 product for 2004–2015 (see Fig. 1 for pixel

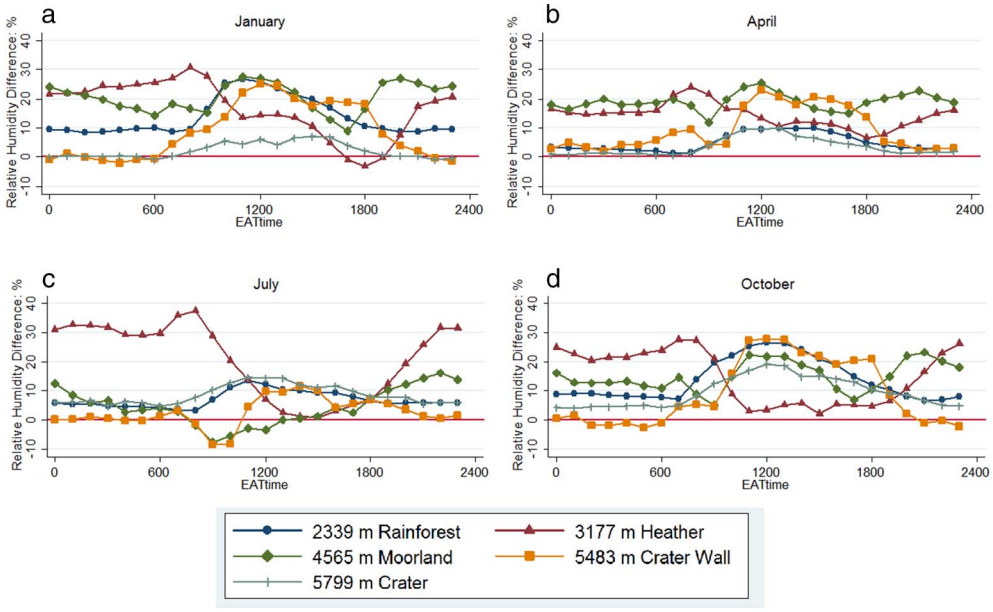

Fig. 9. Seasonal differences in diurnal patterns of slope differences (SW minus NE slope) in relative humidity (%) for a) January, b) April, c) July and d) October. Format similar to Fig. 8.

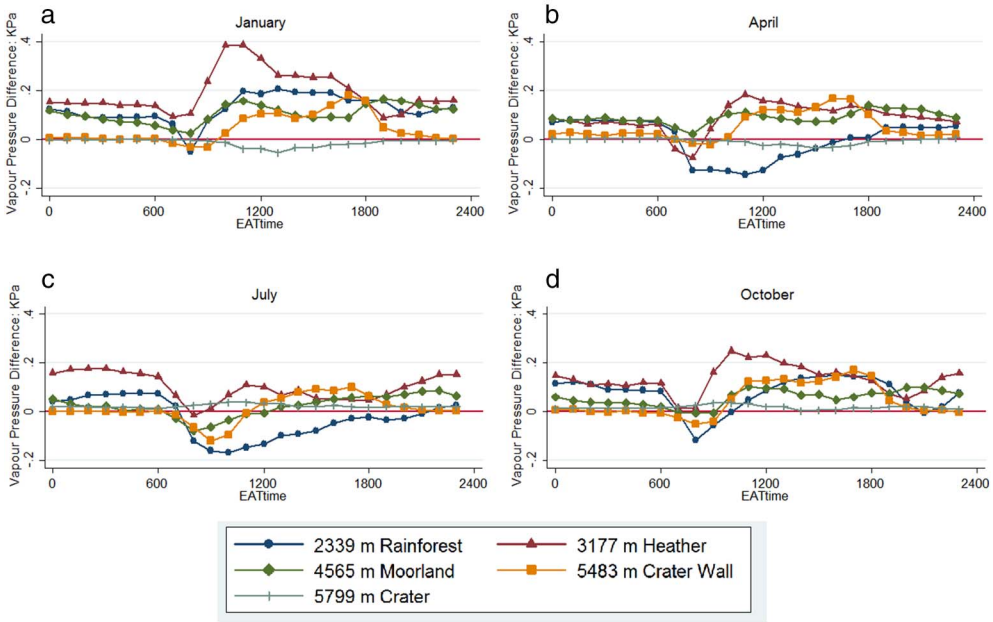

Fig. 10. Seasonal differences in diurnal patterns of slope differences (SW minus NE slope) in vapour pressure (kPa) for a) January, b) April, c) July and d) October. Format similar to Fig. 8.

locations). Tables 2 (0200 EAST) and 3 (1400 EAST) are contingency tables of the frequencies of the number of cloud-free days in each 8-day composite for pixels representing stations on opposing slopes. In this way the extent to which cloud development is synchronous on the two slopes can be quantified. We restrict analysis to stations Mach4/Rong4 (3177 m) just above the rainforest level, and stations Mach9/Rong9 (5464 m) on the crater wall. At night (0200 EAST) the two slopes are generally synchronous (meaning that when there are cloudy conditions on one slope they are also cloudy on the other) and cloudy conditions are relatively rare on both slopes. This is true at both high and low elevations. During the day, cloud presence/absence is typically more synchronous at the upper sites than lower down on the mountain near the rainforest limit. For example, at 1400 EAST at the lower elevation station there are much higher frequencies of cloud cover on the SW slope when the NE slope is intermittently cloudy (represented by frequencies to the right and above the diagonal of the table). However, at the higher station there is much greater correspondence between slopes, apart from when there are no cloud free days on the SW slope (top row) when cloud free conditions are still possible on the NE slope. This suggests that afternoon cloud development at the higher stations is more likely to be on both slopes at the same time rather than lower down the mountain just above rainforest level, where there are distinct differences in simultaneous cloud frequencies between the slopes.

We also analysed our relative humidity data to assess if it was correlated between both slopes (Table 4). On a long term basis the correlation between equivalent elevation stations (station pairs) is significant for all elevations, but r increases above 5000 m – reaching 0.923 at the two summit stations (Albion and Mach10) for the daily mean relative humidity (final column). However, these two stations are close (~200 m apart) because the transects converge and this could therefore be expected. High correlations on the opposing aspects of the crater wall however (e.g. Mach8/Rong8 and Mach9/Rong9 pairings) are not necessarily expected, especially if a typical orographic model is assumed (Roe, 2005), with ascending and descending air on opposing

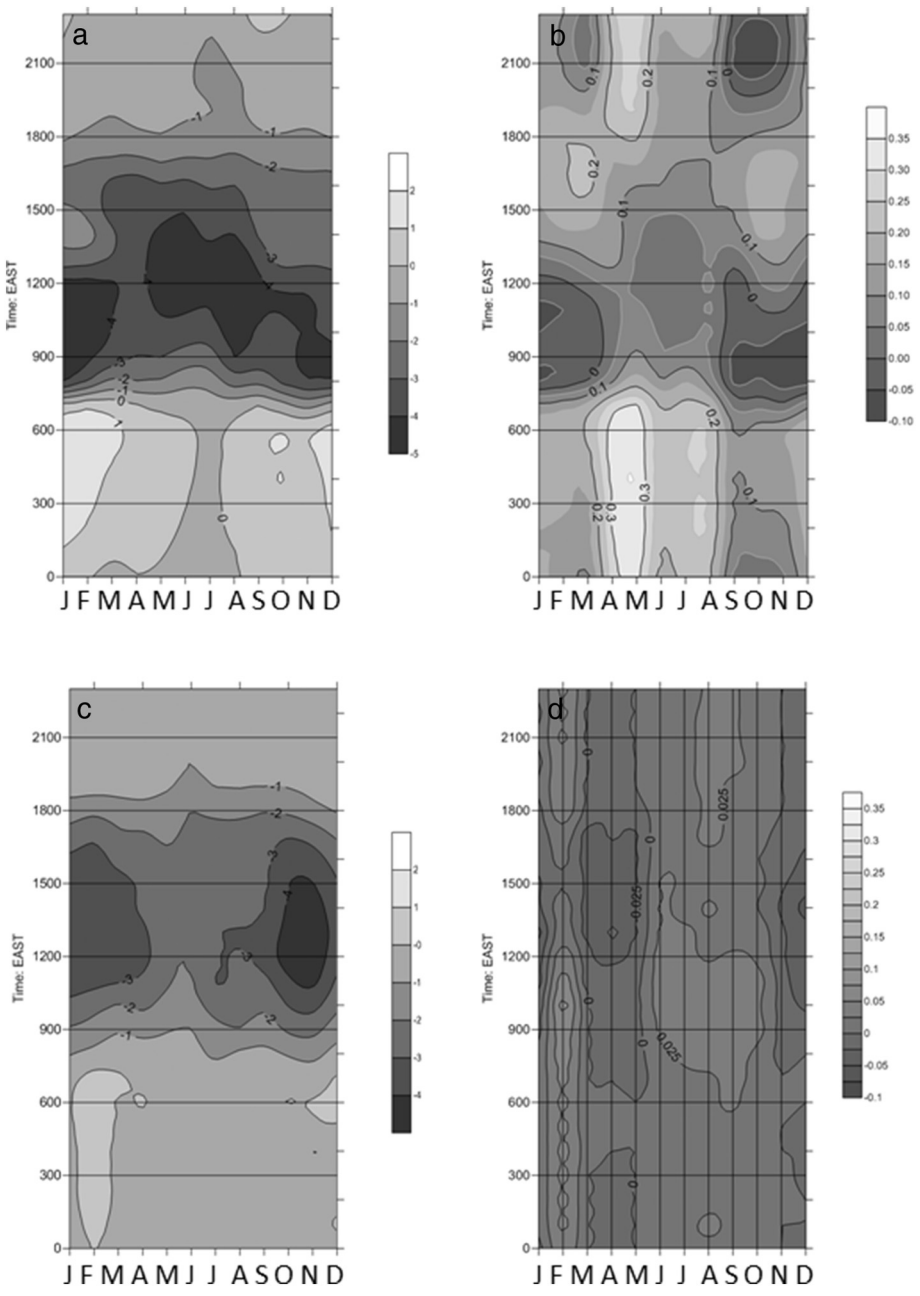

Fig. 11. Local-scale air temperature (left panels: °C) and vapour pressure (right panels: kPa) differences: a) and b) rainforest minus cultivated zone (top row), c) and d) crater ice field minus non-ice station (bottom row). Stations are at approximately the same elevations. Positive/negative differences mean that the rainforest or ice-field is warmer/cooler or moister/drier.

sides of the crater leading to contrasting cloud patterns on either side. However, correlations over 0.9 are common at night.

Table 4 also shows that although night-time humidities are mostly highly correlated (probably driven by common free air moisture content), there is a significant daytime deterioration in correlation (see figures in bold) at many sites. For example, correlations fall below 0.5 at station pairs 7 and 8 between 1100 and 1700 EAST, and also at pair 9 at 1400 EAST. Thus, afternoon convection and upslope moisture entrainment and cloud formation appear to show some decoupling between the two sides of the crater. Some low correlations are also shown lower down the mountain at the upper limit of the rainforest. The lowest correlations are at night at site pairs 3 and 4 (e.g. 0.212 at site 4 at 2000 EAST), suggesting there is often a different nocturnal cloud base level in the vicinity of the treeline on the two sides of the mountain.

Generally similar results appear for correlations on vapour pressures recorded on the two slopes (not shown). Night-time values are mostly strongly correlated between slopes, especially at the higher elevations, suggesting that free atmospheric moisture content is important, whereas daytime values show a dip at all stations, as low as 0.241 at 1100 at pair 4 (3177 m).

3.4. Slope conditions during periods of extensive cloud and/or snowfall at crater level

Because most of the accumulation on the summit ice fields occurs during short periods (Mölg et al., 2009a), case studies of high moisture content at crater level were examined in more detail. Based on webcam analysis at station Mach10 on the NIF, Duane et al. (2008) deemed that relative humidities (RH) above 95% were more likely than not to be associated with the development of cloud cover at the station elevation. The match is not perfect but allows us to estimate a high probability of cloud cover at an individual station when RH is > 95%. Using this assumption, we classify a cloudy hour as 1 and absence of cloud as 0 at each station separately. Adding up all the cloud indices for a slope produces an overall slope cloud index ranging from 0 to 10. Missing data were compensated for, i.e. if only 9 stations recorded data at a particular hour the slope index

Table 2
Contingency table of number of cloud free days in MODIS MYD11A2 composites for 0200 EAST for SW slope (rows) vs NE slope (columns). Bold figures represent similar values on each slope.

a) Station 9 frequency on each slope (5465 m).

NE SW	0	1	2	3	4	5	6	7	Total
0	**1**	0	0	0	0	0	0	0	1
1	0	**1**	0	1	0	0	0	0	2
2	0	0	**4**	2	1	0	0	0	7
3	0	0	3	**14**	2	0	0	0	19
4	0	0	1	9	**33**	8	1	0	52
5	0	0	0	2	15	**56**	8	1	82
6	0	0	0	0	2	24	**109**	6	141
7	0	0	0	0	0	5	38	**159**	202
Total	1	1	8	28	53	93	156	166	506

b) Station 4 frequency on each slope (3177 m)

NE SW	0	1	2	3	4	5	6	7	Total
0	**1**	0	0	0	0	0	0	0	1
1	0	**2**	2	0	0	0	0	0	4
2	0	1	**3**	6	0	2	0	0	12
3	0	2	5	**15**	6	3	1	0	32
4	0	0	2	11	**26**	16	2	0	57
5	0	0	0	1	18	**41**	26	5	91
6	0	0	0	0	3	32	**57**	28	120
7	0	0	0	0	0	8	40	**141**	189
Total	1	5	12	33	53	102	126	174	506

Table 3
Contingency table of number of cloud free days in MODIS MYD11A2 composites for 1400 EAST for SW slope (rows) vs NE slope (columns). Bold figures represent similar values on each slope.

a) Station 9 frequency on each slope (5465 m)

NE SW	0	1	2	3	4	5	6	7	Total
0	**43**	55	51	48	37	18	4	1	257
1	17	**12**	21	19	10	4	3	0	86
2	8	10	**12**	8	7	5	0	0	50
3	5	10	11	**8**	5	9	1	0	49
4	6	5	7	2	**9**	2	3	0	34
5	2	1	2	3	5	**2**	0	0	15
6	0	2	1	3	1	3	**2**	1	13
7	0	0	0	0	0	0	2	**0**	2
Total	81	95	105	91	74	43	15	2	506

b) station 4 frequency on each slope (3177 m)

NE SW	0	1	2	3	4	5	6	7	Total
0	**7**	7	7	2	1	0	0	0	24
1	4	**13**	11	17	5	2	0	0	52
2	0	5	**17**	26	25	15	2	0	90
3	2	7	13	**20**	30	22	7	0	101
4	0	1	6	21	**31**	25	16	2	102
5	0	0	2	3	12	**26**	29	4	76
6	0	0	0	3	4	7	**25**	11	50
7	0	0	0	0	0	4	5	**2**	11
Total	13	33	56	92	108	101	84	19	506

Table 4
Correlations between relative humidity at equivalent elevations on each slope (SW versus NE) – figures in bold are < 0.5.

EAST	0200	0500	0800	1100	1400	1700	2000	2300	Mean Daily
1	0.514	0.579	0.585	0.680	0.676	0.686	0.672	0.533	0.617
2	0.545	0.577	0.549	0.640	0.615	0.673	0.646	0.563	0.625
3	**0.377**	**0.386**	**0.363**	0.540	**0.463**	0.580	**0.433**	**0.305**	0.546
4	**0.492**	0.536	**0.498**	0.532	**0.395**	**0.459**	**0.212**	**0.352**	**0.395**
5	0.679	0.693	0.653	0.503	**0.373**	**0.424**	**0.464**	0.641	0.579
6	0.720	0.766	0.752	0.500	**0.475**	**0.487**	0.519	0.688	0.649
7	0.621	0.664	0.589	**0.319**	**0.302**	**0.339**	**0.381**	0.558	0.519
8	0.808	0.805	0.767	**0.485**	**0.324**	**0.327**	0.666	0.792	0.658
9	0.932	0.929	0.880	0.530	**0.459**	0.536	0.901	0.930	0.805
10	0.954	0.962	0.948	0.866	0.821	0.893	0.941	0.955	0.923

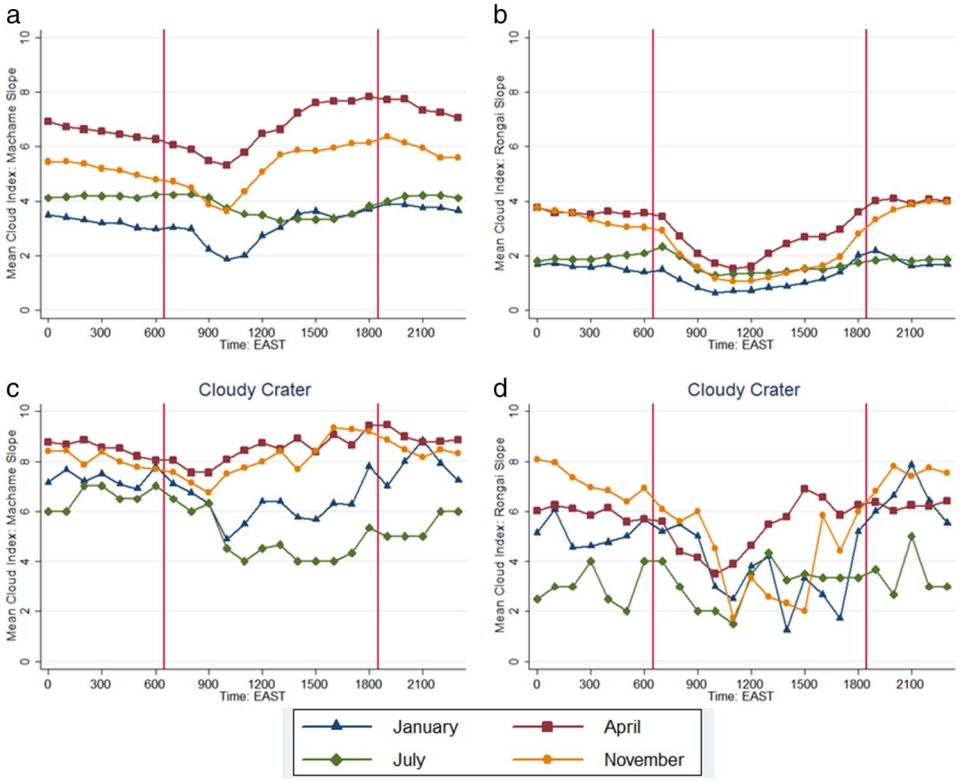

Fig. 12. Diurnal changes in mean cloud index for each slope: a) climatological mean (SW slope), b) climatological mean (NE slope), c) occasions with cloud cover at crater level only (SW slope), d) occasions with cloud cover at crater level only (NE slope). The cloud index shows the number of stations (scaled to between 0 and 10) recording relative humidity > 95% at any one time.

Table 5
Cross-tabulation between cloud indices on each slope (defined by number of stations with relative humidity above 95%). Chi-squared $X^2 = 0.000$. Bold values represent the same cloud index on each slope.

	Rongai											
Mach	0	1	2	3	4	5	6	7	8	9	10	Total
0	**1280**	297	68	7	6	0	2	1	0	0	0	1661
1	773	**233**	133	201	21	2	6	1	0	0	0	1370
2	983	909	**300**	214	54	6	11	4	1	0	0	2482
3	1382	1515	1023	**430**	183	11	50	30	9	1	0	4634
4	1131	1108	1296	917	**477**	113	91	47	17	5	0	5202
5	271	300	389	247	169	**134**	58	15	5	2	0	1590
6	513	467	662	598	431	112	**200**	117	46	18	5	3169
7	321	293	303	352	341	141	286	**178**	84	41	11	2351
8	192	162	179	171	181	116	210	216	**143**	104	39	1713
9	132	118	91	87	133	55	119	165	175	**157**	113	1345
10	6	18	26	32	42	19	58	97	127	149	**154**	728
Total	6984	5420	4470	3256	2038	709	1091	871	607	477	322	26245

was multiplied by a factor of 10/9 for that hour only. Therefore an index of 10 means that RH is above 95% at all (available) stations, and a value of 1 at 10% of stations (usually one station).

Mean cloud indices for each slope are plotted against time of day and season (month) in Fig. 12. The top row shows long term average cycles in cloud frequency for the January and July dry seasons and long (April) and short (November) rains for the SW (panel a) and NE slope (panel b). As expected, the SW slope is cloudier and values are higher in the wet seasons, particularly the long rains when cloud is widespread. The diurnal cycle is such that there is an early morning minimum in cloud extent occurring between the persistent stratiform cloud of the night (particularly on lower slopes) and the afternoon convective cloud which forms after midday. The morning minimum appears strongest on the SW slope and during January. Cloud development during the afternoon is weakest during July. The NE slope also shows a morning minimum but slightly later and there is weaker and slower convective development during the afternoon. The bottom panels (Fig. 12c and d) show the same information but only for occasions when cloud is reported in the crater at the ice field station. This shows much higher cloud amounts all over the mountain, particularly on the SW slope. Thus, crater level cloud formation is not divorced from wider scale development and moistening of the whole mountain. This is particularly true in the wet seasons. In the July dry season, however, it is possible for a cloudy crater to be surrounded by a less cloudy mountain, particularly during the afternoon (typical cloud indices around 4 on SW and 2–4 on NE slope).

It is also of interest to look at a contingency table between the cloud indices calculated for each slope (based on > 95% RH) (Table 5). In general there is a strong correlation (chi squared value is highly significant at < 0.001), but on many occasions the SW slope has higher values than the NE, whilst it is very unusual for the opposite to occur. When the NE slope is extremely cloudy (9 or 10) then it is likely that the SW is as well. Thus, there is a high correspondence between extreme moisture/cloudy episodes on the two sides of the mountain.

Finally, mean daily cloud indices are also calculated for each station based on the number of hours with RH > 95%. A cloudy hour is given a value of 1, and non-cloudy −1. The values are summed over a 24 hour period (midnight to midnight). Table 6 lists daily cloud indices

Table 6
Mean daily cloud indices for days with and without snowfall at crater Albion station (5794 m). The p value shows the significance of the difference in mean cloud index at each station. Cloud indices were calculated by taking the average of the 24 hourly values (1 = cloud present, −1 = cloud absent, 0 = missing data). A value of zero therefore means that 50% of the day has cloud cover, and a negative value < 50%.

Mean cloud index	1100 EAST		
	No snowfall (n = 1051)	Snowfall (n = 40)	p value
Moshi	−0.60	−0.52	0.203
Mbahe	−0.48	−0.40	0.394
Mach1	0.33	0.59	0.038*
Mach2	0.65	0.81	0.092
Mach3	0.52	0.80	0.003*
Mach4	0.15	0.55	0.0001*
Mach5	−0.25	0.25	0.000*
Mach6	−0.14	0.05	0.004*
Mach7	−0.33	0.23	0.000*
Mach8	−0.51	−0.44	0.000*
Mach9	−0.75	−0.32	0.000*
Mach10	−0.73	−0.26	0.000*
Albion	−0.73	−0.26	0.000*
Rong9	−0.65	−0.39	0.0004*
Rong8	−0.63	−0.38	0.001*
Rong7	−0.70	−0.21	0.000*
Rong6	−0.39	−0.17	0.005*
Rong5	−0.50	−0.09	0.000*
Rong4	−0.60	−0.28	0.0001*
Rong3	−0.15	0.46	0.000*
Rong2	−0.07	0.39	0.000*
Rong1	−0.69	−0.31	0.000*

* Significant difference at 0.05.

at each station for days reporting significant snowfall at crater level (change in surface snow cover from no snow to snow as measured by reflected radiation – see Methods) compared with all other days. Since significant snowfall is quite rare, the number of snowfall days (n = 40) is much lower than the non-snowfall category. In all cases (i.e. at all stations) the mean cloud index is higher for snowfall days, and this difference is significant at all stations on the NE slope, and above Mach2 (2340 m) on the SW slope. Thus, snowfall at crater level is associated with significantly more cloudy conditions across nearly the whole mountain.

4. Discussion

The basic differences in temperature and vapour pressure between the two slopes (NE slope warmer and less humid than the SW on average) are as would be expected due to contrasts in both land cover and solar loading due to aspect/latitude. First, since the SW slope has a much denser and vertically extensive rainforest zone, this will both depress air temperatures due to the protective effect of the canopy, and increase vapour pressure, particularly during the daytime due to increased latent heat flux. It is therefore unsurprising that large amounts of cooling (up to 5 °C) and increases in vapour pressure (up to 0.25 kPa) are found at elevations representative of the rainforest (2000–3000 m) and part of the giant heather zone (3000–3500 m) immediately above.

Second, there is also a large cooling effect found higher up the mountain at around 5000–5500 m which at least in part can be related to shading effects. The SW slope at 5000 m is protected from incoming sunlight until around 0900 EAST by the crater wall and the cooling effect at this elevation will therefore be largest during the hours immediately following sunrise. By late afternoon the SW slope faces the sun and the NE slope is in shadow and eventually the SW slope becomes slightly warmer (1700 EAST at 5500 m, for example). Most of the time however, increased afternoon cloudiness keeps the SW slope cool, thus corroborating the early findings of Meyer (1891) and Gillman (1923) who recognised the unequal distribution of glaciers on Kilimanjaro (lower extent on the SW slope) as a response to increased afternoon cloud cover. Our data shows that the moisture content over most of the SW slope is increased throughout most of the day, but there is an exception in the morning in some areas. This is again a result of aspect effects as the rising sun would start evaporation earlier on the NE slope, leading to a slightly drier SW slope atmosphere for a short period (a couple of hours) after sunrise. In summary, observed slope differences can be explained by a combination of land-cover and aspect driven effects, the latter becoming more important at the higher elevations where vegetation becomes minimal and the slopes are steeper.

We also examined the differences in temperature and vapour pressure within the crater (ice versus no ice) and at the rainforest edge on the SW slope. Temperature differences were seen to be of broadly similar magnitude to those reported between slopes (i.e. a cooling of up to 4–5 °C). Thus, it is likely that vegetation differences contribute in part to the slope differences in temperature. The same is broadly true for vapour pressure differences, although in this case the difference due to the rainforest within the SW slope (Fig. 11b) can be slightly larger than differences observed between slopes (Fig. 5b). This implies that without differences in vegetation, the NE slope could have been more humid than the SW. Since the NE (windward) slope is exposed to free-atmospheric moisture this is not unsurprising. Clearly differences in vegetation are a reasonable explanation for much of the existing contrast between the two slopes of the mountain.

In addition, the ice fields induce local scale cooling on the crater of 3–4 °C in the afternoon, acting as a heat sink (increased latent heat flux). Although mean air temperatures recorded at Mach10 on the NIF average around −6 °C during 2012–2015 from our data and −7 °C from AWS3 on the crater rim during 2005–2007 (5873 m) (see Mölg et al., 2008), daytime temperatures recorded away from this ice field are often 3–4 °C warmer (Fig. 11c). Although still below freezing for the majority of the time, this brings afternoon air temperatures much nearer to the 0 °C threshold and therefore more significant melting could conceivably occur in future given modest warming coupled with the expected reduction of the heat sink effect as the ice fields recede.

Beyond differences in slope climatology, we are also interested in the synchronicity or lack thereof in moisture transport on the two slopes on a synoptic timescale. Since day-to-day contrasts in vapour pressure on the two slopes are highly correlated this suggests that large scale advective influences are important in controlling moisture availability on the mountain, in particular free atmospheric changes as a result of synoptic disturbances (Hastenrath, 2001; Chan et al., 2008). On occasions when variance is decoupled on the mountain sides, this is evidence that local scale mountain phenomena are also at work. In general, inter-slope correlations across the three-year period (Table 4) are high, meaning that there are significant common synoptic controls, corroborating the findings of Mölg et al. (2009a) and Chan et al. (2008) that extensive heavy precipitation events tend to be associated with widespread moistening of the free atmosphere. However, the strongest correlations occur at night and not in the daytime when most precipitation would be expected to fall in a traditional convective regime. The high values over 0.9 for relative humidity and vapour pressure at high elevation stations (> 5000 m) on opposing sides of the crater during night time hours are notable. Examination of the diurnal cycle of precipitation on the summit crater would be informative here but such data is as yet unavailable.

The strong coupling between slopes sometimes reduces, most importantly during the afternoon when differential solar heating of the two slopes (and therefore differential moisture stores) appear to induce differential amounts of upslope moisture transport. The lowest correlations between mean daily vapour pressure on the two slopes are seen at the rainforest limit (around 2800–3200 m), showing that a depression in the treeline on the NE slope, in comparison with the SW slope, influences moisture availability most profoundly at that elevation. During the afternoon, however, the zone of greatest decoupling moves upslope to around 4500–5000 m, meaning that differences between slopes become apparent in the daytime moisture regime in the alpine

desert. Even at 5500 m, the afternoon moisture patterns are different on the two sides, but to a lesser extent. In many debates about summit moisture supply (Mölg et al., 2009a, 2012) there are traditionally thought to be two moisture sources, that of the free atmosphere (influenced by SSTs in the Indian Ocean), and that of the lower slopes of the mountain (influenced by land-cover). In reality it might be more complex than this as each slope can behave independently of the other on occasion. There are also additional un-instrumented slopes in between our measurements (the mountain is a cone) for which there is no information. For continued presence of the ice fields, there could be advantage in diversity of moisture sources for maintaining mass balance as slope contrasts could in theory act as a buffer for change (i.e. when one source is reduced another could compensate). More research is required to determine whether this has occurred in reality.

It is also important to compare the observed decoupling of the relative humidity and cloud regimes on the slopes with the modelling results of Mölg et al. (2009a). In Mölg et al. (2009a), the typical 'flow-around' regime induces convection on the leeward slope and the upslope flow of moisture on the SW slope is shown to be dynamically forced. However, the extent to which moisture in this upward flow is influenced by upwind free-atmospheric moisture content, as opposed to moisture from the leeward slope itself, is unanswered. Our observations do not contradict this model of dynamic forcing, but because slope decoupling in moisture content is strongest during the afternoon, this suggests that moisture on the leeward slope itself may supplement any upwind source carried around the mountain from the NE slope.

Notwithstanding the afternoon decoupling of relative humidity regimes, cloud patterns on the two slopes as demonstrated through use of the MODIS cloud mask, however, appear to be fairly well correlated both by day and night. During the afternoon (Table 3), the low level stations may be somewhat decoupled, but the higher elevations are much more consistent. Thus cloud tends to be reported on both slopes at the same time by MODIS, even though relative humidity readings can become decoupled. The reasons for this require more research. MODIS cloud mask data (which records cloud cover at or above the station) is not the same as in situ humidity data (which records cloud solely at station level).

Finally, a disproportionately large number of moist events with heavy snowfall at crater level are associated with high humidity at all other points and extensive cloud, both for the slope as a whole (Table 5), and at most individual stations (Table 6). Thus, significant humidity/precipitation events at crater level that create snow accumulation do not occur in isolation, but usually moisten the whole mountain, which adds support to the role of widespread free-air disturbances in supplying moisture to the crater level (Chan et al., 2008).

Our comprehensive analysis of moisture patterns on the mountain allows us to make comments relevant to the debate about the effect of deforestation on the summit ice fields. We find evidence both to support and to refute the hypothesis that deforestation is an important control. On the supporting side, the increased moisture recorded on the SW (forested) slope in comparison with the NE (less-forested) slope extends all the way to crater level, and the fact that local-scale differences between forested/non-forested sites are broadly similar to larger-scale differences between slopes supports the idea that differences in land-cover have a strong influence both on local climate and in creating these slope differences on a regional scale. The upslope moisture transport is also clearly stronger and more rapid on average on the forested SW slope than on the NE slope. Thus if forest on the SW slope was removed it would have a significant effect not only on in situ conditions, but also on upslope moisture transport. On the other hand, the fact that heavy snow accumulation at crater level is associated with increased moisture all over the mountain (rather than strongly correlated with individual slope moisture sources) implies that slope contrasts cannot solely account for summit precipitation contrasts under the specific synoptic conditions leading to substantial accumulation events at crater level.

In a modelling study, Mölg et al. (2012) simulated the effect of deforestation (land cover change - LCC) on the mass balance of the summit ice fields and glaciers and found that the various ice masses, e.g. SIF and NIF, behaved in different ways. Although the main conclusion was that there was "limited forcing of glacier loss (p. 1)", there certainly were changes for individual ice-masses, albeit not consistent. On the south side of the mountain, the Kersten glacier, "suffered additional seasonal mass loss in the range 0–27% due to LCC since the 1970s (p. 2)", not an insignificant change. However for the other summit ice masses, including the NIF, the change was less consistent, and even an increase in mass balance due to LCC could not be ruled out. This implies that different parts of the summit could be influenced by different precipitation regimes. The justification given by Mölg et al. (2012) was that highly-localised moisture convergence zones accounted for most precipitation at high elevations. Such zones could shift position due to LCC and thus lead to heterogeneous outcomes across the crater. Our findings which suggest that NIF snowfall is associated with widespread cloud cover across the mountain may initially appear to go against the highly localised nature of high intensity events, but observations of widespread cloud cover do not mean that during such events the relative density of moisture content (and precipitation) could not still be dependent on specific moisture sources, which in turn would impact the overall amount of snowfall and influence its exact spatial signature. Clearly, any interpretation of our observations in this context requires more thought, and a detailed comparison with model simulations is highly recommended.

5. Summary and conclusions

We summarise our main findings as follows:

- Both slopes of the mountain show an upward transport of moisture from the lower slopes during the afternoon but this process is weaker and delayed on the NE slope compared to the SW slope (Figs. 4, 6).
- The SW slope is much cooler (up to 4–5 °C) and moister (up to 0.2 kPa) than the NE slope at an equivalent elevation. Temperatures are reduced most strongly in the first half of the day (Fig. 5a).
- Aspect differences on the crater wall create opposing differences in temperature and moisture content at around 5000–5500 m in the early morning (NE warmer and moister) and late afternoon (SW warmer and moister) (Fig. 5a).
- There is a temporary moisture deficit on the SW slope during the morning because evaporation starts earlier on the NE slope. This reverses in the afternoon (Fig. 5b).
- The largest differences in vapour pressure, relative humidity and cloud between the slopes tend to be around the upper limit of the rainforest (~3100–3200 m), both in cloud development during the daytime and in the level of the nocturnal cloud base (Fig. 7).
- Seasonal changes in the slope differences are subtle but in general, differences are bigger and more variable in the dry seasons (Figs. 8–10).
- Local scale differences in temperature due to forest (up to 3–4 °C) and vapour pressure (up to 0.3 kPa) within the SW slope are roughly of similar magnitude to the differences between slopes (Fig. 11a and b). Ice field differences (up to 3–4 °C and 0.03 kPa) are similar for temperature, but much smaller for vapour pressure (Fig. 11c and d).
- Daytime cloud development on the upper slopes tends to be more synchronous than lower down the mountain (Table 3). Night time cloud formation tends to be synchronous at all levels (Table 2).
- The relative humidity regimes are highly correlated on the two slopes at night, particularly on the crater walls, but some differences emerge on the higher slopes during the afternoon (Table 4). Very cloudy conditions on both slopes tend to occur at the same time (Table 5).
- For periods characterised by high humidity and cloud development at the crater, there is often extensive cloud development over the whole mountain, but particularly on the SW slope and in the wet

seasons (Fig. 12). Thus, moist periods at the crater do not occur in isolation from the rest of the mountain. Days with snowfall at crater level are also significantly more cloudy at nearly all sites on both mountain slopes (Table 6).

This paper presents the basic patterns of observed moisture variability on opposing slopes of Kilimanjaro, and further work is required to compare these with detailed model simulations (Mölg et al., 2009a; Fairman et al., 2011; Mölg et al., 2012). In particular, there is a need to understand the effects of local scale land-cover change on the hydrological cycle in a mountainous context (Lambrechts et al., 2002), including the consequences for agriculture and population on the lower slopes (Hemp, 2005; Soini, 2005).

Although only 3 years of data are used in this paper, currently our observations on the SW slope extend back to 2004, and those on the NE back to 2012. A longer record and more extensive observations from across the mountain is critical to allow us to validate future model simulations but also to gain a better appreciation of inter-annual variability due to synoptic factors such as El-Niño Southern Oscillation, examine temperature trends at a range of elevations to identify elevation-dependent warming (e.g. Pepin et al., 2015), and increase our understanding of the longer-term interactions inherent within tropical mountain ecosystems.

Acknowledgements

We thank NERC (Natural Environment Research Council) for providing funding (NE/J013366/1) for fieldwork on Kilimanjaro and the expansion of the weather station network to cover the north-eastern slope. We thank Doug Hardy, Mark Losleben, Andrew Day, Simon Mtuy and staff at Summit Expeditions and Nomadic Experience for help in the field over the years. We thank COSTECH, TANAPA and KINAPA for help with the necessary permits. Kilimanjaro air temperature and humidity data for 2012–2015 is archived with NERC at the Centre for Environmental Data Analysis http://catalogue.ceda.ac.uk/uuid/57116a45a09847a68395c75362436e05. We thank Eduardo Maeda for help with Fig. 1 and for extracting the MODIS MYD11A2 cloud mask data retrieved from the online Data Pool, courtesy of the NASA Land Processes Distributed Active Archive Center (LP DAAC), USGS/Earth Resources Observation and Science (EROS) Center, Sioux Falls, South Dakota, https://lpdaac.usgs.gov/data_access/data_pool. There are no conflicts of interest.

References

Altmann, J., Alberts, S.C., Altmann, S.A., 2002. Dramatic change in local climate patterns in the Amboseli basin, Kenya. Afr. J. Ecol. 40, 248–251.
Appelhans, T., Mwangomo, E., Otte, I., Detsch, F., Nauss, T., Hemp, A., 2016. Eco-meteorological characteristics of the southern slopes of Kilimanjaro, Tanzania. Int. J. Climatol. 36, 3245–3258.
Bohleber, P., Sold, L., Hardy, D., Schwikowski, M., Klenk, P., Fischer, A., Sirguey, P., Cullen, N.J., Potocki, M., Hoffmann, H., Mayewski, P., 2016. Ground-penetrating radar reveals ice thickness and undisturbed englacial layers at Kilimanjaro's Northern Ice Field. Cryosphere. http://dx.doi.org/10.5194/tc-2016-154.
Bridges, R.C., 1976. W.D. Cooley, the RGS and African geography in the nineteenth century: part I: Cooley's contribution to the geography of eastern Africa. Geogr. J. 142, 27–47.
Camberlin, P., Phillipon, N., 2002. The east African March–May rainy season: associated atmospheric dynamics and predictability over the 1968–97 period. J. Clim. 15, 1002–1019.
Chan, R.Y., Vuille, M., Hardy, D.R., Bradley, R.S., 2008. Intraseasonal precipitation variability on Kilimanjaro and the East African region and its relationship to the large-scale circulation. Theor. Appl. Climatol. 93, 149–165.
Cook, K.H., Vizy, E.K., 2013. Projected changes in East African rainy seasons. J. Clim. 26, 5931–5948. http://dx.doi.org/10.1175/JCLI-D-12-00455.1.
Cooley, W.D., 1852. Inner Africa Laid Open in an Attempt to Trace the Chief Lines of Communication Across That Continent, Longman, Brown, Green and Longmans, second edition. 1969 Negro Universities Press, New York.
Coutts, H.H., 1969. Rainfall of the Kilimanjaro area. Weather 24, 66–69.
Cullen, N.J., Mölg, T., Kaser, G., Hussein, K., Steffen, K., Hardy, D.R., 2006. Kilimanjaro: recent areal extent from satellite data and new interpretation of observed 20th century retreat rates. Geophys. Res. Lett. 33, L16502. http://dx.doi.org/10.1029/2006GL0227084.
Cullen, N.J., Mölg, T., Hardy, D.R., Steffen, K., Kaser, G., 2007. Energy-balance model validation on the top of Kilimanjaro, Tanzania, using eddy covariance data. Ann. Glaciol. 46, 227–233.
Cullen, N.J., Sirguey, P., Mölg, T., Kaser, G., Winkler, M., Fitzsimons, S., 2013. A century of ice retreat on Kilimanjaro: the mapping reloaded. Cryosphere 7, 419–431.
Daly, C., Neilson, R.P., Phillips, D.L., 1994. A statistical-topographic model for mapping climatological precipitation over mountainous terrain. J. Appl. Meteorol. 33, 11–38.
Duane, W.J., Pepin, N.C., Losleben, M.L., Hardy, D.R., 2008. General characteristics of temperature and humidity variability on Kilimanjaro, Tanzania. Arct. Antarct. Alp. Res. 40, 323–334.
Fairman Jr., J.G., Nair, U.S., Christopher, S.A., Mölg, T., 2011. Land use change impacts on regional climate over Kilimanjaro. J. Geophys. Res. Atmos. 116, D03110.
Findlater, J., 1977. Observational aspects of the low-level crossequatorial jet stream of the western Indian Ocean. Pure Appl. Geophys. 115, 1251–1262.
Gillman, C., 1923. An ascent of Kilimanjaro. Geogr. J. 61, 1–27.
Hastenrath, S., 1991. Climate Dynamics of the Tropics. Kluwer, Dordrecht, Boston, London.
Hastenrath, S., 2001. Variations of East African climate during the past two centuries. Clim. Chang. 50, 209–217.
Hastenrath, S., Greischar, L., 1997. Glacier recession on Kilimanjaro, East Africa, 1912–89. J. Glaciol. 43, 455–459.
Hemp, A., 2005. Climate change-driven forest fires marginalize the impact of ice cap wasting on Kilimanjaro. Glob. Chang. Biol. 11, 1013–1023.
Hemp, A., 2006. Vegetation of Kilimanjaro: hidden endemics and missing bamboo. Afr. J. Ecol. 44, 305–328.
Kaser, G., Hardy, D.R., Mölg, T., Bradley, R.S., Hyera, T.M., 2004. Modern glacier retreat on Kilimanjaro as evidence of climate change: observations and facts. Int. J. Climatol. 24, 329–339.
Kaser, G., Mölg, T., Cullen, N.J., Hardy, D.R., Winkler, M., 2010. Is the decline of ice on Kilimanjaro unprecedented in the Holocene? The Holocene 20, 1079–1091.
Kuemmel, B., 1997. Temp, humidity and dew point ONA. http://www.faqs.org/faqs/meteorology/temp-dewpoint/, Accessed date: 7 May 2007.
Lambrechts, C., Woodley, B., Hemp, A., et al., 2002. Aerial Survey of the Threats to Mt. Kilimanjaro Forests. UNDP, Dar es Salaam.
Meyer, H., 1890. Ascent to the summit of Kilima-Njaro. Proc. R. Geogr. Soc. 12, 331–345.
Meyer, H., 1891. Across East Africa Glaciers. G. Philip and Son, London.
Mölg, T., Hardy, D.R., 2004. Ablation and associated energy balance of a horizontal glacier surface on Kilimanjaro. J. Geophys. Res. Atmos. 109.
Mölg, T., Kaser, G., 2011. A new approach to resolving climate-cryosphere relations: downscaling climate dynamics to glacier-scale mass and energy balance without statistical scale linking. J. Geophys. Res. Atmos. 116.
Mölg, T., Hardy, D.R., Kaser, G., 2003. Solar-radiation-maintained glacier recession on Kilimanjaro drawn from combined ice-radiation geometry modeling. J. Geophys. Res. Atmos. 108.
Mölg, T., Cullen, N.J., Hardy, D.R., Kaser, G., Klok, L., 2008. Mass balance of a slope glacier on Kilimanjaro and its sensitivity to climate. Int. J. Climatol. 28, 881–892.
Mölg, T., Cullen, N.J., Hardy, D.R., Winkler, M., Kaser, G., 2009a. Quantifying climate change in the tropical mid troposphere over East Africa from glacier shrinkage on Kilimanjaro. J. Clim. 22, 4162–4181.
Mölg, T., Chiang, J.H.C., Gohm, A., Cullen, N.J., 2009b. Temporal precipitation variability versus altitude on a tropical high mountain: observations and mesoscale atmospheric modeling. Q. J. R. Meteorol. Soc. 135, 1439–1455.
Mölg, T., Cullen, N.J., Kaser, G., 2009c. Solar radiation, cloudiness and longwave radiation over low-latitude glaciers: implications for mass-balance modelling. J. Glaciol. 55 (190), 292–302.
Mölg, T., Kaser, G., Cullen, N.J., 2010. Glacier loss on Kilimanjaro is an exceptional case. Proc. Natl. Acad. Sci. 107, E68.
Mölg, T., Grosshauser, M., Hemp, A., Hofer, M., Marzeion, B., 2012. Limited forcing of glacier loss through land cover change on Kilimanjaro. Nat. Clim. Chang. 2, 254–258. http://dx.doi.org/10.1038/nclimate1390.
Pepin, N.C., Seidel, D.J., 2005. A global comparison of surface and free-air temperatures at high elevations. J. Geophys. Res. 110, D03104. http://dx.doi.org/10.1029/2004JD005047.
Pepin, N.C., Duane, W.J., Hardy, D.R., 2010. The montane circulation on Kilimanjaro, Tanzania and its relevance for the summit ice fields: comparison of surface mountain climate with equivalent reanalysis parameters. Glob. Planet. Chang. 74, 61–75.
Pepin, N., Duane, W., Schaefer, M., Pike, G., Hardy, D., 2014. Measuring and modeling the retreat of the summit ice fields on Kilimanjaro, East Africa. Arct. Antarct. Alp. Res. 46, 905–917.
Pepin, N., Bradley, R.S., Diaz, H.F., Baraer, M., Caceres, E.B., Forsythe, N., Fowler, H., Greenwood, G., Hashmi, M.Z., Liu, X.D., Miller, J.R., Ning, L., Ohmura, A., Palazzi, E., Rangwala, I., Schöner, W., Severskiy, I., Shahgedanova, M., Wang, M.B., Williamson, S.N., Yang, D.Q., 2015. Elevation dependent warming in mountain regions of the world. Nat. Clim. Chang. 5 (5), 424–430.
Pepin, N.C., Maeda, E.E., Williams, R., 2016. Use of remotely-sensed land surface temperature as a proxy for air temperatures at high elevations: findings from a 5000 metre elevational transect across Kilimanjaro. J. Geophys. Res. Atmos (ISSN 2169-897X). http://dx.doi.org/10.1002/2016JD025497.
Prinz, R., Nicholson, L., Mölg, T., Gurgiser, W., Kaser, G., 2016. Climatic controls and climate proxy potential of Lewis Glacier, Mt. Kenya. Cryosphere 10, 133–148. http://dx.doi.org/10.5194/tc-10-133-2016.
Richner, H., Phillips, P.D., 1984. A comparison of temperatures from mountaintops and the free atmosphere: their diurnal variation and mean difference. Mon. Weather Rev. 112, 1328–1340.
Roe, G.H., 2005. Orographic precipitation. Annu. Rev. Earth Planet. Sci. 33, 645–671.
Røhr, P.C., Killingtveit, Å., 2003. Rainfall distribution on the slopes of Mt Kilimanjaro. Hydrol. Sci. J. 48, 65–77.
Schär, C., 2002. Mesoscale mountains and the larger scale atmospheric dynamics: a review. In: Pearce, R.P. (Ed.), Meteorology at the Millennium. Academic Press, New York, pp. 29–42.
Schuler, L., Hemp, A., Behling, H., 2014. Relationship between vegetation and modern

pollen-rain along an elevational gradient on Kilimanjaro, Tanzania. The Holocene 24 (6), 702–713.
Shongwe, M.E., van Oldenborgh, G.J., van den Hurk, B., van Aalst, M., 2011. Projected changes in mean and extreme precipitation in Africa under global warming. Part II: East Africa. J. Clim. 24, 3718–3733.
Soini, E., 2005. Land use change patterns and livelihood dynamics on the slopes of Mt. Kilimanjaro, Tanzania. Agric. Syst. 85, 306–323.
Climate change 2013: the physical science basis. In: Stocker, T.F., Qin, D., Plattner, G.-K., Tignor, M., Allen, S.K., Boschung, J., Nauels, A., Xia, Y., Bex, V., Midgley, P.M. (Eds.), Contribution of Working Group I to the Fifth Assessment Report of the Intergovernmental Panel on Climate Change. Cambridge University Press, Cambridge, United Kingdom and New York, NY, USA.
Troll, C., Wien, K., 1949. Der Lewisgletscher am Mount Kenya. Geogr. Ann. 31, 257–274.
Whiteman, C.D., 1990. Observations of thermally developed wind systems in mountainous terrain. In: Atmospheric Processes over Complex Terrain, Meteor. Monogr. No. 45. Amer. Meteor. Soc., pp. 5–42.
Whiteman, C.D., Hubbe, J.M., Shaw, W.J., 2000. Evaluation of an inexpensive temperature datalogger for meteorological applications. J. Atmos. Ocean. Technol. 17 (1), 77–81.
Winkler, M., Kaser, G., Cullen, N.J., Mölg, T., Hardy, D.R., Pfeffer, W.T., 2010. Land-based marginal ice cliffs: focus on Kilimanjaro. Erdkunde 179–193.